The Carnot efficiency between these temperatures is:

$$1 - \left(\frac{273 + 140}{273 + 314}\right) = 0.296$$

This provides an absolute upper limit to the Rankine cycle efficiency.

Hence, it follows:

Heat Absorbed from Stream 3	= 46.2 MW
Power Produced by Steam Turbine	= 13.7 MW
Required Power Output of Gas Turbine	= 51.3 MW
For the Gas Turbine Cycle Calculated for Case 2,	
Upper Exhaust Temperature T_6 of Figure 10(b)	= 384.7°C
Cycle Efficiency	= 0.4058
For Power Output of 51.3 MW,	
Heat Input to Cycle	= 126.4 MW
Heat Available in Exhaust (0.6 MW Assumed Lost in Transmission)	= 74.5 MW

Making the "best case" assumption that pivot P_2 moves down to 140°C as the exhaust flowrate is reduced:

$$\text{Heat in Exhaust Below } 140°\text{C} = 74.5 \times \frac{(140 - 25)}{(384.7 - 25)}$$

$$= 23.8 \text{ MW}$$

Heat Required by Process Below Equivalent Interval Boundary Temperature = 8.5 MW

$\therefore$ Heat Rejected to Ambient = 23.8 − 8.6 = 15.2 MW

In the Best "Gas Turbine Only" Case, Heat Rejected to Ambient = 22.6 MW

Energy Saved = 22.6 − 15.2 = 7.4 MW

or 4.3% Improvement.

This size of improvement is not large enough to justify the installation of a steam cycle alongside the gas turbine cycle.

LITERATURE CITED

Christodoulou, K., Diploma Thesis, N.T.U., Athens, Greece (1982).

Ichikawa, S., "Use of Fluorocarbon Turbine in Chemical Plants," *Chem. Economy and Eng. Rev.* (Oct., 1970).

Linnhoff, B., "Thermodynamic Analysis in the Design of Process Networks," PhD Thesis, Leeds (1979).

Linnhoff, B., and E. Hindmarsh, "The Pinch Design Method for Heat Exchanger Networks," *Chem. Eng. Sci.* 38, No. 5, 745 (1982).

Linnhoff, B., D. R. Mason, and I. Wardle, "Understanding Heat Exchanger Networks," *Comp. and Chem. Eng.*, 3, No. 1–4, special issue on 214th event of E.F.C.E., Montreux (1979).

Linnhoff, B., and J. A. Turner, "Simple Concepts in Process Synthesis give Energy Savings and Elegant Designs," *Chem. Eng.*, 742 (Dec., 1980).

Sega, K., "Freon Turbine," *Chem. Economy and Eng. Rev.*, 6, 8, 27 (1974).

Stephanopoulous, G., Personal Communication Referring to This Manuscript (1982).

Su, J. L., "A Loop-Breaking Evolutionary Method for the Synthesis of Heat Exchanger Networks," M.S. Thesis, Washington University (1979).

Manuscript received February 25, 1982; revision received October 5, and accepted October 20, 1982.

Studies in Magnetochemical Engineering

Part II: Theoretical Development of a Practical Model for High-Gradient Magnetic Separation

High-gradient magnetic separation (HGMS) is an existing commercial technology which promises to be an effective means for the large-scale separation of both weakly magnetic and practically nonmagnetic, micron-sized particles. It utilizes the strong magnetic forces created typically by placing filamentary ferromagnetic packing materials inside a separator matrix magnetized by a uniform background magnetic field. In this paper, a practical mathematical model for HGMS is developed for quantitatively predicting the grade and recovery of the separated product and the capacity (concentration breakthrough) of the separator. Computer implementation and experimental verification of the new model for HGMS applied to pilot-scale coal beneficiation are described in Part III.

Y. A. LIU

Department of Chemical Engineering
Virginia Polytechnic Institute and State University
Blacksburg, VA 24061

and

M. J. OAK

Department of Chemical Engineering
Auburn University
Auburn University, AL 36849

SCOPE

HGMS is an existing commercial technology which has extended the applicability of magnetic methods from separating the small class of strongly magnetic (ferromagnetic) materials to the much larger class of very weakly magnetic (weakly paramagnetic) materials. The technology is also applicable to separating nonmagnetic (diamagnetic) materials which can be made to associate with magnetic seeding materials. It was developed around 1969 for the wet separation of the weakly

Part I of this series appeared in *Fuel*, 58, 245 (1979).

Correspondence concerning this paper should be addressed to Y. A. Liu. M. J. Oak is with the Department of Chemical Engineering, Princeton University, Princeton, NJ 08544.

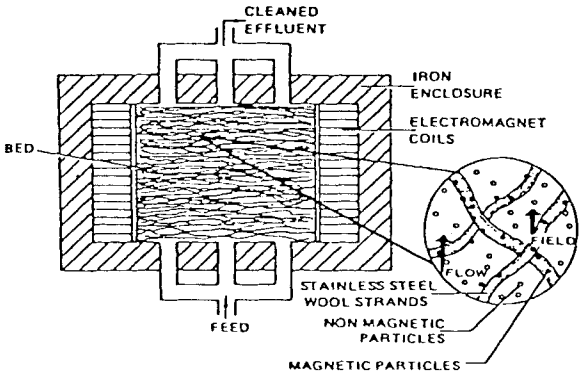

Figure 1. A schematic diagram of a typical HGMS unit (Oder, 1976; © 1976, IEEE).

magnetic contaminants from kaolin clay to improve its brightness for use in paper coating (Luborsky, 1975).

A typical HGMS unit in this wet application consists of a cylindrical separator matrix packed loosely with fine strands of ferromagnetic stainless-steel wool and magnetized by a strong uniform background magnetic field (Figure 1). The matrix packing materials increase and distort the background field in their vicinity, thus creating many tiny regions in the separator matrix where the spatial variations of the field intensity (called field gradients) are highly significant. The resulting high-gradient magnetic fields generate very strong magnetic forces which enable the matrix to capture fine particles of very low magnetic susceptibilities.

In a typical wet application, the feed slurry containing weakly magnetic contaminants is pumped through the magnetized separator matrix from the bottom while the magnet is on. The magnetic materials (mags) are captured and retained inside the separator matrix and the nonmagnetic components (tails) pass through the separator matrix and are collected as the beneficiated producted from the top of the matrix. After some time of operation, the separator matrix is saturated with attracted magnetic materials. The feed is then stopped, and the separator matrix is rinsed with water. Finally, the magnet is turned off, and the mags retained inside the separator matrix are backwashed with water and collected as a magnetic refuse stream. The whole procedure is repeated in a cyclic fashion.

Large-scale commercial HGMS units like that shown in Figure 1 are being used worldwide to beneficiate over 4 million tons of kaolin clay per year. Because of its very low costs and outstanding technical performance demonstrated in the kaolin application, HGMS is being adopted to solving many separation problems related to the chemical and minerals processing industries. Successful commercial applications of HGMS to such areas as mineral beneficiation, solid reclamation and catalyst recovery have already been reported. Detailed discussion of the basic principles of HGMS, design features of laboratory and industrial HGMS units, and potential and industrial applications of HGMS can be found elsewhere (Liu, 1979).

The technical performance of HGMS is generally characterized by the grade and recovery of the separated product, and by the capacity (concentration breakthrough) of the separator. Recent theoretical and experimental studies for quantitatively characterizing the technical performance of HGMS have been reviewed (Luborsky, 1975; Birss and Parker, 1981). The reported studies show that the technical performance of HGMS depends on how efficiently the separator matrix captures magnetic particles (particle capture) and how much of the captured particles can be retained in the separator matrix (particle buildup). Several of the existing models based on particle capture and buildup provide a useful means for quantitative correlations of the effects of certain separation variables such as field intensity and slurry velocity on the grade and/or recovery of the separated product.

However, none of these models has been shown to be applicable to quantitatively predicting the effects of a wide range of separation variables on the grade, recovery and concentration breakthrough observed in pilot-scale experimental studies of HGMS. In addition, most of the reported model and experimental studies of HGMS has been limited only to the feed streams containing either pure magnetic particles or simple mixtures of magnetic and nonmagnetic particles of approximately monodispersed or narrowly distributed size. Little attention has been devoted to relating the technical performance of HGMS to the characteristic of the feed stream containing a wide range of sizes, densities and magnetic susceptibilities. Also, a number of modeling studies have examined the effects of mechanical entrapment on the technical performance of HGMS at low or zero field intensities. However, for separations at high field intensities, particularly those involving very fine, weakly magnetic particles, the effect of mechanical entrapment can often be neglected.

The objective of this study is to develop a practical mathematical model which can be used to quantitatively predict the grade, recovery and concentration breakthrough observed in pilot-scale experimental studies of HGMS. Specifically, the technical performance of HGMS is quantitatively examined by first considering the relative importance of the capture and buildup of magnetic particles in the separator matrix under the commonly used separation conditions for wet HGMS processes. Special attention is devoted to relating the technical performance of HGMS to the characteristic of the feed stream. A practical HGMS model based on the particle buildup and feed characteristic is then proposed and illustrated with simple applications. The computer implementation and experimental verification of the new model for HGMS applied to pilot-scale coal beneficiation are described in Part III.

CONCLUSIONS AND SIGNIFICANCE

This work presents a detailed quantitative study of the technical performance of HGMS and proposes a new practical model applicable to separations involving feed streams of a wide range of sizes, densities and magnetic susceptibilities under the commonly used separation conditions for wet HGMS processes. Specifically, in this paper and in Part III, the new practical model based on the particle buildup and feed characteristic is shown to be applicable to quantitatively predicting the grade, recovery and concentration breakthrough observed in pilot-scale experimental studies of HGMS applied to coal beneficiation. Based on the theoretical developments and computational results presented, the following major conclusions and significance of the present work can be summarized.

1. The technical performance of HGMS is quantitatively related to the particle capture and buildup. Under the commonly used separation conditions for wet HGMS processes, however, the capability of the separator matrix to capture magnetic particles remains practically unchanged and essentially all magnetic particles are captured before the matrix is saturated or loaded with the buildup of particles. As a result, there is practically no need to quantitatively characterize the particle capture. The main factor is determining the technical performance of a pilot-scale or an industrial HGMS unit appears to be the particle buildup, and not the particle capture.

2. Both the particle capture and buildup are highly dependent upon the dimensionless ratio of the so-called magnetic velocity V_m (Watson, 1973) to the free stream fluid velocity V_∞. Here, the magnetic velocity V_m is essentially a terminal velocity of a particle in a magnetic field. It is defined by:

$$V_m = \frac{2\mu_o M H_o \chi R^2}{9\eta a}$$

Except for the length L and packing void fraction ϵ of the separator matrix, the ratio V_m/V_∞ is shown to contain almost all of the major independent variables in HGMS: (a) particle properties—size R and magnetic susceptibility χ; (b) flow field—fluid viscosity η and free stream fluid velocity V_∞; (c) magnetic field—field intensity H_o and magnetization of wire M (μ_o is the permeability of the free space); and (d) separator matrix packing characteristic—wire radius R (and magnetization M). The maximum amount of particle buildup on the separator matrix packing wire increases with increasing value of V_m/V_∞, and there exists a minimum magnetic velocity, $V_{m,\min}$, for the captured particles to remain sticking to the wire matrix. This minimum magnetic velocity can be uniquely determined from experimentally measurable variables in HGMS.

3. Under conditions of constant magnetic and flow fields and of fixed separator matrix packing characteristic, the magnetic velocity V_m is mainly a function of particle properties. To quantitatively relate the technical performance of HGMS to the characteristic of the feed stream containing particles of a wide range of sizes, densities and magnetic susceptibilities, it is necessary to determine the magnetic velocities of particles in the feed stream and the distribution of such velocities. These magnetic velocity distributions can be readily determined from the particle-size measurement of the feed stream and from simple analyses of samples obtained from a standard float-and-sink separation of the feed stream. By incorporating such magnetic velocity distributions determined prior to actual magnetic separation testing, the new particle buildup model developed in this work can be used to quantitatively predict the grades, recoveries and concentration breakthrough curves of specific magnetic particles of interest in HGMS.

In this paper, a practical mathematical model is developed for predicting the experimentally observed grade, recovery and concentration breakthrough in pilot-scale HGMS units, Figure 1. The basic principles of HGMS, design features of laboratory and industrial HGMS units, and the potential and industrial applications of HGMS can be found in Liu (1979). The published review of Birss and Parker (1981) as well as a recent article in this journal by Gooding and Felder (1981) also contain excellent introductory descriptions of HGMS. Technical performance of HGMS is quantitatively examined here by first considering both particle capture and buildup under the presently used or proposed conditions for wet HGMS processes. Special attention is devoted to relating the technical performance of HGMS to the characteristic of the feed stream. A practical HGMS model based on the particle buildup and feed characteristic is then proposed and illustrated with simple applications.

PARTICLE CAPTURE AND BUILDUP IN HGMS

The theoretical analysis of the capture of a magnetic particle by the magnetized, ferromagnetic collecting wire in the separator matrix of an HGMS unit can be viewed as two separate, but related, problems. First, one can consider the motion of the particle by analyzing its trajectory in the magnetic field, and determine under what conditions a particle will strike the wire. Secondly, after the impact of a particle on the wire, one can examine whether the particle will stick to the wire and continue to build up as a layer on the surface of the wire with other attracted particles, or the particle will be washed away from the wire by the fluid. Much of the recent analyses of the first problem (for example, Luborsky, 1975) follows the analogous work by Zebel (1965) concerning the deposition of an aerosol particle flowing past a cylindrical fiber in a uniform electric field and is briefly reviewed below. In addition, some theoretical extensions of these recent analyses along with their practical implications are also presented.

Particle Capture (Trajectory) with Buildup of Particles

Consider a ferromagnetic wire of radius a and magnetization M placed axially along the x-axis in the coordinate system shown in Figure 2a. A uniform magnetic field H_o, which is strong enough to saturate the wire, is applied in the positive x-direction. A fluid

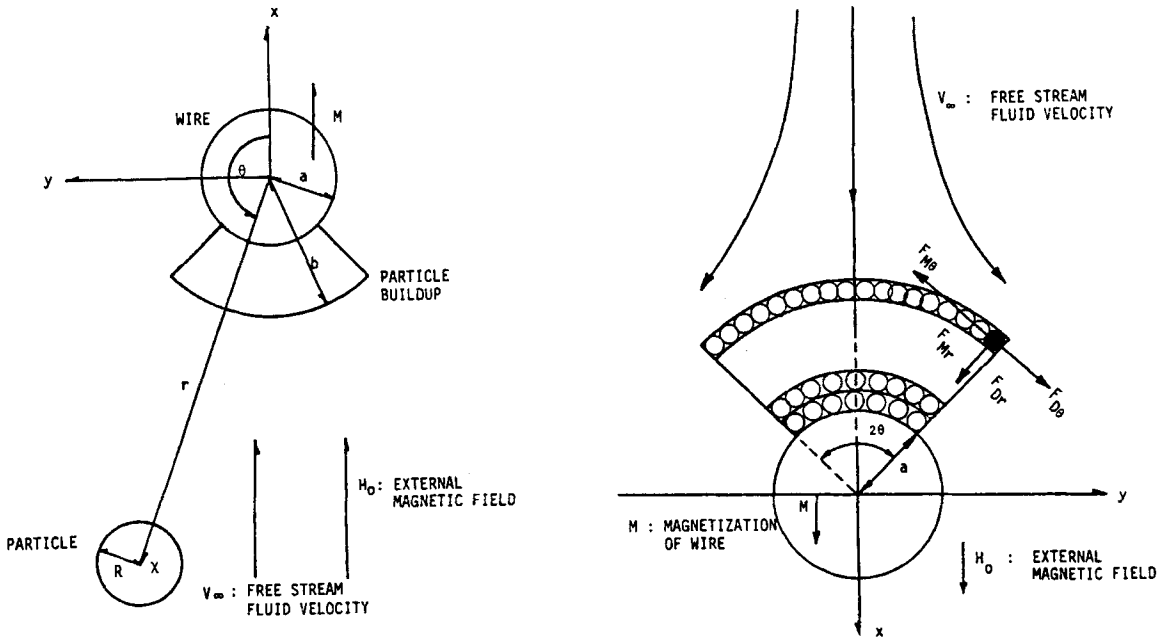

Figure 2. The coordinate systems used for (a) particle trajectory calculation (left) and (b) particle buildup calculations (right).

of viscosity η is flowing past the wire in the same direction with a free stream velocity V_∞. The fluid carries a paramagnetic particle of radius R and magnetic susceptibility χ. The particle is initially located on angle θ with respect to the x-axis and a distance r from the origin. Particles previously attracted are assumed to have been built up on the wire in a cylindrical configuration (Himmelblau, 1973; Cowen et al., 1976a,b) with radius b; the flow field around the wire is approximated by the potential flow. Also, to simplify the modeling efforts, the effect of particle buildup on magnetic field is assumed to be practically negligible as was done in all previous modeling studies. With these simplifying assumptions, the motion of the particle can be described by the following force balance equations, Appendix A in Part III.

(r-component)

$$0 = \frac{V_m}{V_\infty}\left(\frac{a^3}{r^3}\right)\left\{\frac{Ma^2}{2H_o r^2} + \cos 2\theta\right\} - \left\{\left(1 - \frac{b^2}{r^2}\right)\cos\theta - \frac{1}{V_\infty}\frac{dr}{dt}\right\}$$

(MAGNETIC) (DRAG)

$$+ \left(\frac{2R^2}{9\eta V_\infty}\right)(\rho_p - \rho_f)g\cos\theta - \left(\frac{2\rho_p R^2}{9\eta V_\infty}\right)\left\{-\frac{d^2r}{dt^2} + r\left(\frac{d\theta}{dt}\right)\right\} \quad (1)$$

(GRAVITY) (INERTIAL)

(θ-component)

$$0 = \frac{V_m}{V_\infty}\left(\frac{a^3}{r^3}\right)\sin 2\theta - \left\{\left(1 + \frac{b^2}{r^2}\right)\sin\theta - \frac{r}{V_\infty}\frac{d\theta}{dt}\right\}$$

(MAGNETIC) (DRAG)

$$- \left(\frac{2R^2}{9\eta V_\infty}\right)(\rho_p - \rho_f)g\sin\theta - \left(\frac{2\rho_p R^2}{9\eta V_\infty}\right)\left\{-r\frac{d^2\theta}{dt^2} - 2\frac{dr}{dt}\frac{d\theta}{dt}\right\} \quad (2)$$

(GRAVITY) (INERTIAL)

In Eqs. 1 and 2, V_m is called the magnetic velocity (Watson, 1973) as defined by:

$$V_m = \frac{2\mu_o M H_o \chi R^2}{9\eta a} \quad (3)$$

It has the unit of velocity such as cm/s, and can be considered as a terminal velocity of a particle in the magnetic field. The dimensionless group V_m/V_∞ appearing in Eqs. 1 and 2 contains most of the major independent variables in HGMS: (a) particle properties—size R and magnetic susceptibility χ; (b) flow field—fluid viscosity η and free stream fluid velocity V_∞; (c) magnetic field—field intensity H_o and magnetization of wire M; and (d) separator matrix packing characteristic—wire radius R (and magnetization M).

Both Eqs. 1 and 2 can be solved numerically to yield the particle trajectory for a given set of parameters and initial conditions. Under the commonly used separation conditions for wet HGMS processes, however, the results of an order-of-magnitude analysis of different force terms (for example, Birss and Parker, 1981, pp. 183–186) can be used to simplify Eqs. 1 and 2 and allow them to be solved analytically. First, for separations of fine particles in a liquid slurry at a slow velocity, the gravity and inertial forces are normally negligible compared to the magnetic and drag forces. Secondly, in the expressions for the latter two forces in Eqs. 1 and 2, there are three short-range terms, namely $Ma^2/2H_o r^2$, $-b^2\cos\theta/r^2$ and $b^2\sin\theta/r^2$. These terms are inversely proportional to r^2. As a result, their magnitudes may be considered to be negligible when a particle is far away from the wire ($r \gg a$ or b).

Consider the first simplified case when the short-range term $Ma^2/2H_o r^2$ and the gravity and inertial forces in Eqs. 1 and 2 are neglected (Luborsky and Drummond, 1975). Equations 1 and 2 can be combined to give

$$\frac{1}{r_a}\frac{dr_a}{d\theta} = \frac{\left(1 - \frac{b_a^2}{r_a^2}\right)\cos\theta - \left(\frac{V_m}{V_\infty}\right)\left(\frac{1}{r_a^3}\right)\cos 2\theta}{-\left(1 + \frac{b_a^2}{r_a^2}\right)\sin\theta - \left(\frac{V_m}{V_\infty}\right)\left(\frac{1}{r_a^3}\right)\sin 2\theta} \quad (4)$$

where the reduced variables $r_a = r/a$ and $b_a = b/a$. By defining an additional reduced coordinate, $y_a = y/a$, Eq. 4 can be used to relate explicitly the trajectory of a particle entering at an initial coordinate $y_a = y_\infty$ at $x = -\infty$ according to

$$y_a^\infty = r_a\left(1 - \frac{b_a^2}{r_a^2}\right)\sin\theta - \left(\frac{V_m}{2V_\infty}\right)\left(\frac{1}{r_a^2}\right)\sin 2\theta \quad (5)$$

Equation 5 does not represent properly the particle trajectory at the so-called singular points in the magnetic field. At those points, the differential quotient (Eq. 4) assumes an indeterminate value of 0/0. The latter implies physically that the magnetic and drag forces on the particle exactly compensate each other. The particle can thus remain at the singular points indefinitely. This equilibrium of forces is, however, an unstable one; any small disturbance will lead the particle to a neighboring trajectory where it moves away from the singular point (Zebel, 1965). The specific initial reduced coordinate, for which the particle is just captured by the wire, is called the critical entering coordinate and denoted by R_c. From Eqs. 4 and 5, R_c is given by (Luborsky and Drummond, 1975):

$$R_c = \begin{cases} \left(\frac{V_m}{2V_\infty}\right)\left(\frac{1}{b_a^2}\right) & \text{if } \frac{V_m}{V_\infty} \le \sqrt{2}b_a^3 \quad (6a) \\ \text{constant of singularity} & \text{if } \frac{V_m}{V_\infty} > \sqrt{2}b_a^3 \quad (6b) \end{cases}$$

The constant of singularity in Eq. 6b can be calculated by simultaneously solving the expressions obtained from equating the numerator and the denumerator of Eq. 4 to zero. To avoid the complexity of calculations involved in such a singular situation, it is often desirable to neglect all the three short-range terms and the gravity and inertial forces in Eqs. 1 and 2. The resulting simplified trajectory equation and its analytical solution can be written from Eqs. 4 and 5, respectively, as

$$\frac{1}{r_a}\frac{dr_a}{d\theta} = \frac{\cos\theta - \left(\frac{V_m}{V_\infty}\right)\left(\frac{1}{r_a^3}\right)\cos 2\theta}{-\sin\theta - \left(\frac{V_m}{V_\infty}\right)\left(\frac{1}{r_a^3}\right)\sin 2\theta} \quad (7)$$

$$y_a^\infty = r_a\sin\theta - \left(\frac{V_m}{2V_\infty}\right)\left(\frac{1}{r_a^2}\right)\sin 2\theta \quad (8)$$

The corresponding expression for the critical entering coordinate, R_c, is

$$R_c = \begin{cases} \text{maximum of } y_a^\infty & \text{if } \frac{V_m}{V_\infty} \le 1.0 \quad (9a) \\ \frac{3\sqrt{3}}{4}\left(\frac{V_m}{V_\infty}\right)^{1/3} & \text{if } \frac{V_m}{V_\infty} > 1.0 \quad (9b) \end{cases}$$

For a clean wire without particle buildup ($b_a = b/a = 1$), a good approximation to the maximum of y_a^∞ in Eq. 9a is the linear relationship (Zebel, 1965; Watson, 1973; Luborsky, 1975):

$$R_c = \frac{V_m}{2V_\infty} \quad \text{for} \quad \frac{V_m}{V_\infty} \le \sqrt{2} \quad (10)$$

In Figure 3a, Eqs. 9b and 10 are compared with the results obtained from the exact numerical solutions of Eqs. 1 and 2 neglecting the gravity and inertial forces. This comparison suggests that except when V_m/V_∞ is very small, Eqs. 9b and 10 appear to provide satisfactory approximations to the exact values of R_c as functions of V_m/V_∞.

The above approximations (Eqs. 9b and 10) for R_c for the case of a clean wire can be properly extended to include the effect of particle buildup. For convenience, the actual particle buildup volume on the upstream side divided by the wire volume will be called the relative buildup volume, denoted by f. In Figure 2b, f is the ratio of the volume of hollow cylindrical shell ABCD to that of cylindrical wire ABE. A total buildup angle of $2\theta = \pi/2$ (Figure 2b), as has been observed experimentally (Himmelblau, 1973; Cowen et al., 1976a,b), is assumed; other simplifying assumptions previously leading to Eq. 7 are also made. The critical entering coordinate R_c can then be approximately related to the relative buildup volume f by

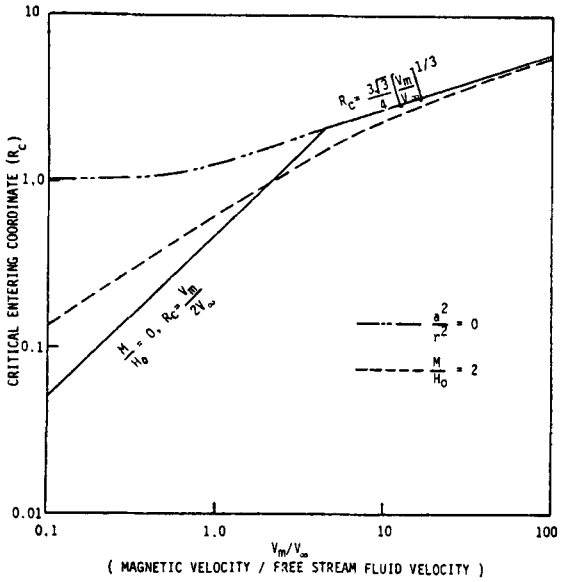

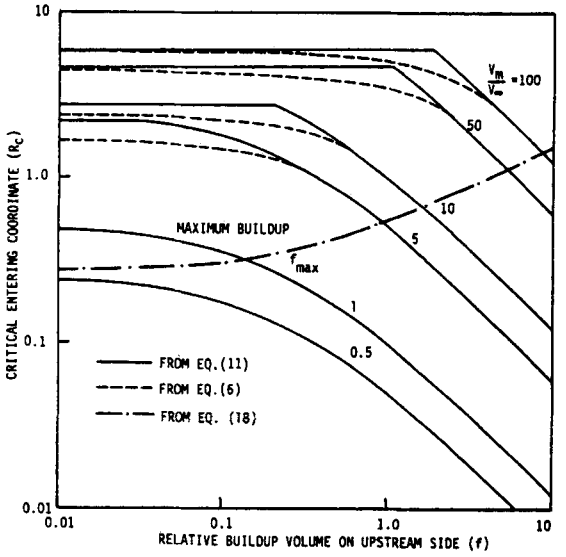

Figure 3. The approximate solution of the critical entering coordinate R_c as a function of (a) the ratio of magnetic velocity to free stream fluid velocity V_m/V_∞ (left) and (b) the relative buildup volume f and maximum buildup volume f_{max} on the upstream side (right).

$$R_C = \begin{cases} \dfrac{V_m}{2V_\infty}\left(\dfrac{1}{4f+1}\right) & \text{if } f \geq f_a \quad (11a) \\ \dfrac{3\sqrt{3}}{4}\left(\dfrac{V_m}{V_\infty}\right)^{1/3} & \text{if } f < f_a \quad (11b) \end{cases}$$

where f_a is

$$f_a = \frac{1}{4}\left\{\frac{2}{3\sqrt{3}}\left(\frac{V_m}{V_\infty}\right)^{2/3} - 1\right\} \quad (11c)$$

Figure 3b shows that Eqs. 11a–11c provide reasonably good approximations to the exact value of R_c obtained from Eqs. 4 and 6a–6b. Also, except during the initial period of particle buildup in which f varies from 0 to 1, Figure 3b and Eq. 11a suggest that the critical entering coordinate R_c is inversely related to the relative buildup volume f. The quantitative dependence of the relative buildup volume on the major independent variables in HGMS is examined below by extending the analysis of Luborsky and Drummond (1976) to consider the equilibrium configuration of particle buildup.

Equilibrium Configuration of Particle Buildup

The equilibrium configuration of the particle buildup can be determined by the balance of forces on the particles as illustrated in the coordinate system of Figure 2b in which only the magnetic and drag forces of importance to the presently used or proposed process conditions for wet HGMS are included. Consider, for example, a particle located in the outermost layer that has been built up cylindrically on the upstream side of the wire. Depending on the size of the particle and the specific flow field assumed, the balance of forces can be examined in two cases as follows.

For relatively large particles, the carrier fluid may pass through the interstices of the particle buildup. By neglecting the effect of the particle buildup on the magnetic and flow fields, and assuming the Stokes' law for the drag force, a force balance on the particle is given by:

(r-component)

$$\frac{4\pi\mu_o\chi M H_o R^3 a^2}{3r^3}\left(\frac{M}{2H_o}\frac{a^2}{r^2} + \cos 2\theta\right) = -6\pi\eta R V_\infty \cos\theta \quad (12)$$

(θ-component)

$$\frac{4\pi\mu_o\chi M H_o R^3 a^2}{3r^3}\sin 2\theta = 6\pi\eta R V_\infty \sin\theta \quad (13)$$

From Eq. 13, the radius of the particle buildup, b, is related to the buildup angle, 2θ (Figure 2b), by

$$b_a = b/a = r/a|_{r=b} = \left(\frac{2V_m}{V_\infty}\right)|-\cos\theta|^{1/3} \quad (14)$$

Substituting Eq. 14 into Eq. 12 yields

$$\left(\frac{2V_m}{V_\infty}\right)\cos^2\theta - b_a^3\cos\theta + \left(\frac{V_m}{V_\infty}\right)\left(\frac{M}{2H_o}\frac{1}{b_a^2} - 1\right) = 0 \quad (15)$$

Equation 15 is a quadratic equation in θ; and its two solutions, θ_1 and θ_2, can be used to define a so-called maximum buildup angle, θ_{max}, as:

$$\theta_{max} = |\theta_1 - \theta_2| \quad (16)$$

The specific maximum buildup angle at $b_a = r/a|_{r=a} = 1$ is also for particular interest in defining the equilibrium configuration of the particle buildup; and it will be called the critical buildup angle, θ_c. This implies that all particles with a buildup angle 2θ greater than θ_c would be swept off by the carrier fluid. Further, as suggested by Luborsky and Drummond (1976), if the tangetial drag force $F_{D\theta}$ is also larger than the tangential magnetic force $F_{M\theta}$, the particle buildup would become unstable. Some of the attracted particles will be washed away from the wire by the carrier fluid.

The integration of the buildup area from $\theta = \pi - \theta_c/2$ to $\theta = \pi$ gives the maximum relative buildup volume on the upstream side of the wire, f_{max}, corresponding to a specific value of θ_c obtained from Eqs. 14 to 16:

$$f_{max} = \frac{1}{\pi}\left(\frac{V_m}{V_\infty}\right)^{2/3}\int_{\pi-\theta_c/2}^{\pi}|-\cos\theta|^{2/3}d\theta - \frac{1}{4} \quad (17)$$

By using the exact value of θ_c obtained from Eqs. 14 to 16 at each value of V_m/V_∞, the maximum relative buildup volume f_{max} computed from Eq. 17 is drawn as a function of V_m/V_∞ in Figure 4a for the two cases with $M/H_o = 0$ and 2. This figure suggests that the maximum amount of particle buildup on the wire increases with increasing value of V_m/V_∞; and there exists a minimum value of V_m/V_∞ for the particles to remain sticking to the wire. For example, at a maximum relative buildup volume of $f_{max} = 1$, the particles having values of V_m/V_∞ less than 6.2 will not be captured on the upstream side of the wire. Also included in Figure 4a is the approximate curve for f_{max} computed by assuming $\theta_c = \pi/2$ for all values of V_m/V_∞. It can be seen that when the magnitude of the short-range term $Ma^2/2H_o r^2$ is negligible, the use of a fixed critical buildup angle of $\theta_c = \pi/2$ satisfactorily approximates the maximum relative buildup volume f_{max} regardless of the value of V_m/V_∞. This approximation will thus be used in the later calculations; Eq. 17 is simplified to:

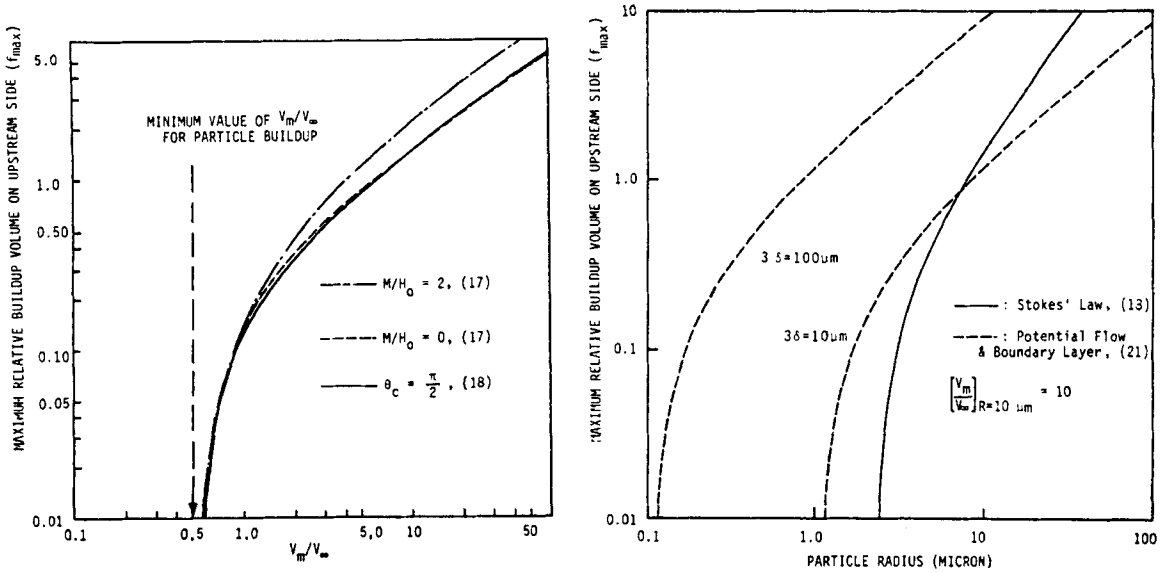

Figure 4. The maximum relative buildup volume of upstream side as a function of (a) the ratio of magnetic velocity to free stream fluid velocity V_m/V_∞ (left) and (b) particle radius (right).

$$f_{max} = \frac{1}{\pi}\left(\frac{V_m}{V_\infty}\right)^{2/3}\int_{3\pi/4}^{\pi}|-\cos\theta|^{2/3}d\theta - \frac{1}{4} \qquad (18)$$

For small particles, the carrier fluid may flow around the boundary of the particle buildup. In this case, an approximate way to represent the flow field is to assume the potential flow around the cylindrical particle buildup, and to include the effect of the fluid boundary layer (Luborsky and Drummond, 1976). The equilibrium configuration of the particle buildup can be determined by a balance of forces on the particle as in Eqs. 12 and 13. For example, the tangential force balance is given by:

$$\frac{-4\pi\mu_o\chi M H_o R^3 a^2}{3r^3}\sin 2\theta = \frac{4\pi R^2\eta}{\delta}V_\infty\sin\theta \qquad (19)$$

where $\delta = (\pi\eta r/V_\infty\rho_f)^{1/2}$ is the fluid boundary layer thickness averaged over the region from $\theta = 3\pi/4$ to $5\pi/4$ (Figure 2b). As in Eq. 14, the radius of the particle buildup can be obtained from Eq. 19 as

$$b_a = \frac{b}{a} = \frac{r}{a}\bigg|_{r=b} = \left(\frac{V_m}{V_\infty}\right)^{1/3}\left(\frac{3\delta}{R}\right)^{1/3}|-\cos\theta|^{1/3} \qquad (20)$$

Similarly, as in Eq. 18 for large particles, an approximate expression for the maximum relative buildup volume on the upstream side of the wire for small particles can be written as:

$$f_{max} = \frac{1}{\pi}\left(\frac{V_m}{V_\infty}\right)^{1/3}\left(\frac{3\delta}{R}\right)^{2/3}\int_{3\pi4}^{\pi}|-\cos\theta|^{2/3}d\theta - \frac{1}{4} \qquad (21)$$

A comparison of the similar expressions (Eqs. 14 and 20; Eqs. 18 and 21) shows that the maximum buildup volume f_{max} is proportional to R for small particles, and to R^2 for large particles. Also, f_{max} is a function of only V_m/V_∞ for large particles; but it is a function of both V_m/V_∞ and δ/R for small particles. In Figure 4b, the maximum relative buildup volumes obtained by using Eqs. 18 and 21 are compared for two cases with $R = 10\ \mu m$, $V_m/V_\infty = 10$, and $3\delta = 10$ and $100\ \mu m$. This figure indicates that the difference in the maximum relative buildup volumes given by Eqs. 18 and 21 depends on the particle size and the value of δ; and this difference is small for large particles. As a result, Eq. 18 can be used to calculate the maximum relative buildup volume for separations involving relatively large particles.

The effect of particle buildup on critical entering coordinate R_c, preciously illustrated in Figure 3b, can now be examined more clearly. For different values of V_m/V_∞, the maximum relative buildup volume f_{max} is calculated by Eq. 18 and included in Figure 3b. It can be seen that for each value of V_m/V_∞, f reaches its maximum value, f_{max}, before R_c begins to decrease significantly. This observation suggests that the capability of the wire to capture particles remains practically unchanged before the wire is saturated or loaded with particles built up on the wire. Thus, before f reaches its maximum value f_{max}, a reasonable approximation is to neglect the variation of R_c with f. The practical implications of this approximation in the modeling of HGMS will be further discussed below.

For the downstream side of the wire, the buildup of particles is highly dependent upon the particle trajectories. In general, an irregular separator matrix packing might increase the possibility of particle capture on the downstream side. It might be suggested that there would be no particles attracted to the downstream side of the wire unless the particles attracted to the upstream side could roll out to the downstream side. Further, most of the particles would be captured on the downstream side after the saturation of particles attracted to the upstream side. In this work, without considering the mechanism of the particle capture on the downstream side, the buildup of particles on the downstream side of the wire is assumed to be the same as that on the upstream side (Himmelblau, 1973; Cowen et al., 1976a; Luborsky and Drummond, 1976). Cowen et al. (1976b), however, have shown experimentally that for the capture and buildup of MnO_2 and α-Fe_2O_3 on a single nickel wire at very low values of V_m/V_∞, the amount of buildup of particles on the downstream of the wire is small. Since no experimental data are presently available on the equilibrium buildup configurations of HGMS of feed streams containing a wide range of sizes, densities and magnetic susceptibilities such as those found in the magnetic beneficiation of coal, it is best to consider the cylindrical buildup of particles on both the upstream and downstream of the collecting wire as assumed in the preceding analysis to be a practical approximation. Further, it should be emphasized that the methodology used in the preceding analysis, as indicated by Eqs. 13 to 21, can be easily modified to account for other equilibrium buildup configurations when future experimental data become available and dictate such a modification.

SEPARATOR PERFORMANCE MODELS

Particle Capture (Trajectory) Model

Consider a thin section of the separator matrix of an HGMS unit of a thickness dx and of a unit cross-sectional area when taken

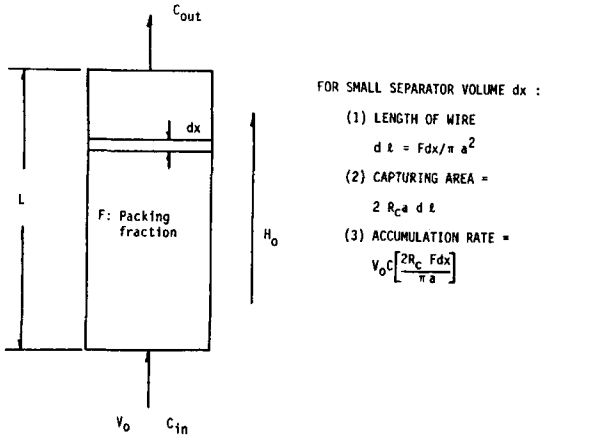

Figure 5. An illustration of the development of the particle capture (trajectory) model.

perpendicular to the magnetic field and fluid flow as shown in Figure 5. Suppose that the fraction of the separator matrix packed with the ferromagnetic particle collecting wires is F, then the related void fraction, denoted by ϵ, as $1 - F$. As the loading capacity, or the amount of particles built up on the wires, is generally limited in HGMS, it is reasonable to neglect the variation of the packed or void fraction with the particle buildup. By referring to Figure 6 and adapting the analysis of Watson (1973), the length of the wire in a thickness dx per unit cross-sectional area of the separator matrix is given by $Fdx/\pi a^2$. The effective cross-sectional area per unit length of the wire for the particle capture is related to the critical entering coordinate R_c by $2R_ca$. This suggests that the total capture cross section which the wire presents to the carrier fluid is $2R_caFdx/\pi a^2$. It is assumed that all the magnetic particles entering within this capture cross-section are attracted and remain sticking to the wire. Further, both the critical entering coordinate and the total capture cross section are considered to be practically unchanged before the wire is saturated with particles built up on the wire. Thus, the material balance of particles over the thin section dx can be written as

$$\epsilon \frac{\partial C}{\partial t} + V_o \frac{\partial C}{\partial x} = -V_o \left(\frac{2R_cF}{\pi a}\right) C \tag{22}$$

Equation 22 is a typically first-order hyperbolic equation; and the method of characteristics (Acrivos, 1956) suggests that it can be simplified to a set of first-order ordinary differential equations by using a new time variable τ defined by

$$\tau = t - \frac{\epsilon x}{V_o} \tag{23}$$

τ represents the time elapsed from a fixed time $\epsilon x/V_o$ at which the fluid, originally entering the separator at $x = 0$, will arrive at a point x in the separator matrix. In order to follow the motion of the particle as it passes through the separator, it is necessary to assume that the variation of τ with the buildup of particles is negligible, and τ can be considered practically constant. Thus, the use of Eq. 23 simplifies Eq. 22 to

$$\left(\frac{dC}{dx}\right)_\tau = -\left(\frac{2R_cF}{\pi a}\right) C \tag{24}$$

where

$$R_c = \begin{cases} \text{constant} & \text{if } \int_0^t Cdt < C_{in}t_o \quad (25a) \\ 0 & \text{if } \int_0^t Cdt \geq C_{in}t_o \quad (25b) \end{cases}$$

In Eqs. 25a and 25b, C_{in} is the concentration of magnetic particles at the inlet of the separator. t_o is the time required for the wire at the inlet of the separator ($x = 0$) to become saturated or loaded with the buildup of particles. It is given by

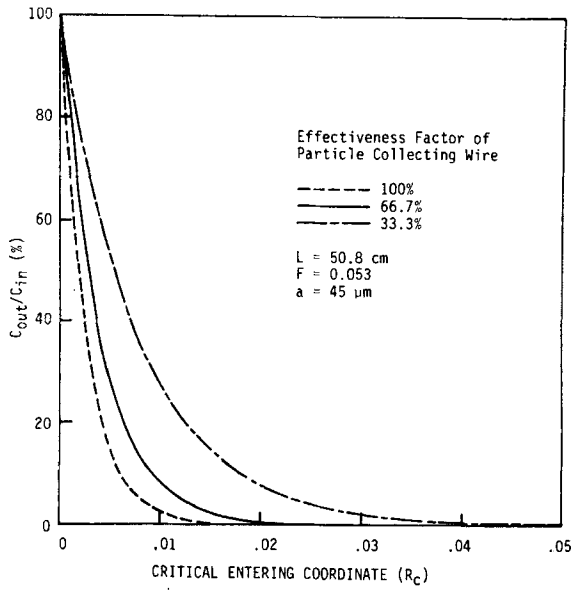

Figure 6. Computed Tail Concentrations of Monodispersed Feed Particles as a Function of the Critical Entering Coordinate Based on the Particle Trajectory Model.

$$t_o = \frac{\pi a f_{max} d}{R_c V_o C_{in}} \tag{26}$$

The integrations of Eqs. 24–26 over the length of the separator matrix L lead to:

$$\frac{C_{out}}{C_{in}} = \exp[-2R_cF(L - x_o)/\pi a] \tag{27}$$

Here, x_o is the length of the saturation zone in the separator matrix defined by

$$x_o = \begin{cases} 0 & \text{if } t < t_o \quad (28a) \\ \dfrac{C_{in}V_o}{2f_{max}Fd}(t - t_o) & \text{if } t \geq t_o \quad (28b) \end{cases}$$

The particle capture (trajectory) model, Eqs. 8 and 26–28b, can be used to estimate the concentration ratios, C_{out}/C_{in}, of magnetic particles in the beneficiated products. Consider, for example, the separation of a slurry of monodispersed magnetic particles in a typical pilot-scale HGMS unit. This separator has a matrix of a total length L of 50.8 cm, a packed fraction F of 0.053, an average wire radius a of 45 μm, and an apparent density of the particle buildup d of 1 g/cm^3. Such length and packing characteristics of the matrix lead to a fairly large exponential factor $2FL/\pi a$ of about 500 in Eq. 27. Further, reported experimental breakthrough curves in HGMS suggest that as the slurry of particles is fed to a separator, there exists an initial period in which the concentration ratio, C_{out}/C_{in}, of magnetic particles in the beneficiated products is practically negligible (Collan et al., 1979). This initial period corresponds to a very short separation zone, $x_o \ll L$, in the separator in which the matrix has not yet become saturated or loaded. When $x_o = 0$ is used to approximate this short separation zone, C_{out}/C_{in}, under the same length and packing characteristics of the matrix considered above, can be calculated as a function of the critical entering coordinate R_c as illustrated in Figure 6. Note that as discussed previously in Eqs. 11a–11b, R_c depends on the ratio V_m/V_∞, which, in turn, is related to essentially all major independent variables in HGMS according to Eq. 3. The rapidly decaying concentration ratio, C_{out}/C_{in}, shown in Figure 6 suggests that even if R_c is very small, almost all magnetic particles will still be captured in the separator matrix. Also included in Figure 6 are two cases corresponding to the wires with effectiveness factors for particle capture being equal to 33.3 and 66.7%, respectively. It is seen that even though the wires are not completely effective in capturing magnetic particles, the concentration ratios in both cases are still practically zero when $R_c > 0.01$.

Based on the preceding development, two practical observations of importance in the quantitative modeling of the performance of HGMS can now be summarized as follows.

(1) The technical performance of HGMS is quantitatively related to the particle capture (trajectory) and buildup. Under the presently used or proposed conditions for wet HGMS processes, however, the capability of the wire matrix to capture magnetic particles remains practically unchanged and essentially all magnetic particles are captured before the matrix is saturated or loaded with the buildup of particles. As a result, there is practically no need to calculate the trajectories of particles along with the critical entering coordinates and the corresponding total capture cross-sections. The main factor in determining the technical performance of a pilot-scale or an industrial HGMS unit appears to be the particle buildup, but not the particle capture (trajectory).

(2) Both the particle capture (trajectory) and buildup are highly dependent upon the magnetic velocity of the particle, V_m. In particular, the maximum amount of particle buildup on the wire increases with increasing value of V_m/V_∞ and there exists a minimum value of V_m/V_∞ for the captured particles to remain sticking to the wire matrix. Under conditions of constant magnetic and flow fields and of fixed separator matrix packing characteristic, the magnetic velocity V_m is mainly a function of particle properties. In order to quantitatively relate the technical performance of HGMS to the characteristics of the feed stream containing particles of a wide range of sizes, densities and magnetic susceptibilities, it is necessary to determine the magnetic velocities of particles in the feed stream and the distribution of such velocities.

Particle Buildup Model Incorporating Feed Characteristic

Based on the above observations, a particle buildup model incorporating the feed characteristic for predicting the technical performance of HGMS under the presently used or proposed conditions for wet separation can be developed by first calculating the minimum magnetic velocity for the captured particles to remain sticking to the wire matrix. The latter is uniquely determined from the following experimentally measureable process variables in HGMS:

(LOAD)= total weight of the captured magnetic particles per unit cross-section of the separator matrix
L= length of the separator matrix
F= packed fraction of the separator matrix ($F = 1 - \epsilon$, where ϵ is the packing void volume fraction)
d= apparent density of the captured magnetic particles retained inside the separator matrix
V_∞= free stream fluid velocity

These definitions suggest that the volume of maximum particle buildup on both upstream and downstream sides divided by the packing wire volume is (LOAD)/LFd. Therefore, the maximum relative buildup volume on the upstream side of the wire matrix, f_{max}, is:

$$f_{max} = \frac{(\text{LOAD})}{2LFd} \tag{29}$$

It then follows from Eq. 18 that the minimum magnetic velocity for particle buildup, $V_{m,min}$ is given by

$$V_{m,min} = 4.45\left[\frac{(\text{LOAD})}{2LFd} + \frac{1}{4}\right]^{3/2} V_\infty \tag{30}$$

Next, a so-called magnetic velocity distribution function for characterizing the feed stream, denoted by $F(V_m)$, is introduced. Specifically, $F(V_m)$ represents the total weight fraction of magnetic particles in the feed stream having a magnetic velocity less than V_m. Thus, if $V_m = V_{m,min}$, $1 - F(V_m)$ corresponds to the total weight fraction of magnetic particles in the feed stream which will be captured inside the separator matrix. This result suggests that a simple particle buildup model incorporating the feed characteristic for HGMS can be written as

$$\frac{C_{out}}{C_{in}} = F(V_m) \qquad V_m = V_{m,min} \tag{31}$$

Here, C_{out} and C_{in} refer to the concentrations of the magnetic particles of interest, such as pyritic sulfur content in the magnetic beneficiation of coal, at the outlet and inlet of the separator matrix, respectively. Further, a simple material balance of particles suggests that (LOAD) can be calculated from the total weight of feed particles per unit cross-section of the separator matrix, (FEED), by integrating the following equation

$$\frac{d(\text{LOAD})}{d(\text{FEED})} = 1 - F(V_m) \qquad V_m = V_{m,min} \tag{32}$$

Characterization of the Magnetic Velocity Distribution. In this work, a systematic procedure has been developed for characterizing the magnetic velocity distribution of the feed stream containing a wide range of sizes, densities and magnetic susceptibilities. This procedure utilizes the readily available data from particle-size determination and standard float-and-sink separation (classic washability analysis) which are commonly used in the analyses of feed streams (particularly their liberation characteristics) in the beneficiation of coal and minerals by physical methods. It can be illustrated with reference to, for example, the application of HGMS to coal beneficiation as described in Part III. In particular, the magnetic velocity distributions for characterizing the pulverized feed coal and its ash, total sulfur and pyrite sulfur components can be quantitatively calculated by the determination of particle-size distribution, a standard float-and-sink separation, and measurements of the magnetic susceptibility along with the ash, total sulfur and pyritic sulfur contents of each separated fraction. Specifically, suppose that $\chi(W)$ and $A_i(W)(i = 1, 2, \text{and } 3)$ are the magnetic susceptibility, and the ash, total sulfur and pyritic sulfur contents, respectively, of the pulverized feed coal at a cumulative weight percent W; and $U(R)$ is the cumulative weight fraction of particles having a radius smaller than R. Under conditions of constant magnetic and flow fields, and of fixed separator matrix packing characteristic, R can be related to the magnetic velocity of the feed stream V_m according to Eq. 3. Thus, in order for particles to have a magnetic velocity less than V_m, the radius of particles with a magnetic susceptibility χ should be smaller than

$$R = \left(\frac{9V_m\eta a}{2\mu_o M H_o \chi}\right)^{1/2} \tag{33}$$

The magnetic velocity distribution of the feed stream, $F(V_m)$, can then be obtained by

$$F(V_m) = \frac{1}{100}\left[\int_{W_o}^{100} U\left\{\left(\frac{9V_m\eta a}{2\mu_o M H_o \chi}\right)^{1/2}\right\} dW + W_o\right] \tag{34}$$

Here, W_o is the weight percent of particles in the feed stream having negative magnetic susceptibilities. Note that implicitly included in Eq. 34 is the practical approximation that except by mechanical entrapment or filtration, no diamagnetic particles will be attracted magnetically by the wire matrix. Based on Eq. 34 and the measurements of ash, total sulfur and pyritic sulfur contents of the pulverized feed coal, the specific magnetic velocity distributions of ash, total sulfur and pyritic sulfur ($i = 1$, 2 and 3, respectively), denoted by $F_i(V_m)$, can be approximated by:

$$F_i(V_m) = \frac{1}{T_i}\left\{\int_{W_o}^{100}\left(\frac{A_i(W)}{100}\right) U\left\{\left(\frac{9V_m\eta a}{2\mu_o M H_o \chi(W)}\right)^{1/2}\right\} dW + \frac{A_{io}W_o}{100}\right. \tag{35}$$

In Eq. 35, T_i, $i = 1$, 2 and 3, are the average ash, total sulfur and pyritic sulfur contents, respectively, of the pulverized feed coal; A_{io}, $i = 1$, 2 and 3, are the average ash, total sulfur and pyritic sulfur contents, respectively, of the fraction W_o with negative magnetic susceptibilities.

Equations 30–35 then represent the new particle buildup model incorporating the feed characteristics for HGMS developed in this

work. This model is a completely *predictive* one, as there is no empirical parameter included in Eqs. 30–35. Further, the distributions of the particle size and density along with the magnetic susceptibility, and the ash, total sulfur and pyritic sulfur contents of each separated fraction after the standard float-and-sink separation used in the model can all be easily measured experimentally *prior to* actual magnetic separation testing. It should also be noted that the method for characterizing the magnetic velocity distribution of the feed stream, as illustrated by Eqs. 30–35 for coal beneficiation, is equally applicable to other HGMS applications such as iron ore beneficiation. In the latter application, for example, one needs only to replace the concentrations of the magnetic particles of interest in the separation from the ash, total sulfur and pyritic sulfur contents in coal beneficiation to the iron oxide content in iron ore beneficiation.

Simple Application of Particle Buildup Model Incorporating Feed Characteristic

As an illustration of the application of the new particle buildup model, one can consider a simple case where all the particles of interest in the feed stream are magnetic with the same positive magnetic susceptibility χ. Further, it is assumed that the cumulative weight fraction of particles having a radius smaller than R, represented by the undersized distribution function $U(R)$, satisfies the following equation:

$$U(R) = 1 - \exp\left[-\left(\frac{R}{m}\right)^n\right] \tag{36}$$

where m and n are known dimensionless size distribution constants. Based on Eq. 3 or 33, the radius of a particle R can be related to its magnetic velocity V_m by the expression

$$R = \left[\frac{9\eta a}{2\mu_o M H_o \chi}\right]^{1/2} V_m{}^{1/2} \tag{37}$$

In order that a particle is captured when the total weight of the magnetic particles captured per unit cross-section of the separator matrix is (LOAD), this particle must have a radius R larger than $R_{\min}$. The latter is specified by substituting $V_{m,\min}$ given by Eq. 30 into 37:

$$\begin{aligned} R_{\min} &= \left[\frac{9\eta a}{2\mu_o M H_o \chi}\right]^{1/2} V_{m,\min}{}^{1/2} \\ &= \left[\frac{9\eta a}{2\mu_o M H_o \chi}\right]^{1/2} \left\{V\left[\frac{(\text{LOAD})}{2LFd} + \frac{1}{4}\right]^{3/2}(4.45)\right\}^{1/2} \end{aligned} \tag{38}$$

Under conditions of known magnetic and flow fields as well as of given feed properties and separator matrix packing characteristic, the only unknown variable in Eq. 38 is (LOAD). The latter can be calculated by integrating Eq. 32 with the magnetic velocity distribution $F(V_m)$ defined by Eq. 34. In particular, since the feed stream contains no particles with negative susceptibilities $W_o = 0$ and the magnetic susceptibility distribution $\chi(W)$ is simply χ (independent of W), $F(V_m)$ as given by Eq. 34 can be simplified as follows:

$$\begin{aligned} F(V_m) &= \frac{1}{100}\int_{W_o}^{100} U(R)dW + \frac{W_o}{100} \\ &= U(R) \\ &= 1 - \exp\left[-\left(\frac{R}{m}\right)^n\right] \end{aligned}$$

Therefore, the total weights of magnetic particles of interest which are captured by and fed to a unit cross-section of the separator matrix, denoted by (LOAD) and (FEED), respectively, can be related by Eq. 32 as follows:

$$\frac{d(\text{LOAD})}{d(\text{FEED})} = 1 - F(V_m) \qquad V_m = V_{m,\min} \tag{32}$$

$$= \exp\left[-\left(\frac{R}{m}\right)^n\right] \qquad R = R_{\min} \tag{39}$$

Note that in Eq. 39, $R_{\min}$ is specified by Eq. 38, which contains only one unknown variable, (LOAD). Therefore, when the known dimensionless size distribution constants m and n are substituted into Eq. 39, and $R_{\min}$ given by Eq. 38 is substituted into Eq. 39 for R, the resulting equation can be readily integrated to give explicitly numerical values of (LOAD) at different values of (FEED). Further, the concentrations of the magnetic particles of interest at the outlet and inlet of the separator matrix, denoted by C_{out} and C_{in}, respectively, can be related by Eq. 31 as follows:

$$\frac{C_{\text{out}}}{C_{\text{in}}} = F(V_m) \qquad V_m = V_{m,\min} \tag{31}$$

$$= 1 - \exp\left[-\left(\frac{R}{m}\right)^n\right] \qquad R = R_{\min} \tag{40}$$

Therefore, once $R_{\min}$ is found from (LOAD) according to Eq. 38 by integrating Eq. 39, C_{out} can be explictly calculated from C_{in} using Eq. 40.

In Part III, the computer implementation and experimental verification of the new model for predicting the technical performance of HGMS applied to pilot-scale coal beneficiation are presented; and the practical applications of the modeling results to the optimum design and operations of HGMS processes for coal beneficiation are also discussed.

Literature Cited and Notation Sections appear at the end of Part III on page 788 of this issue.

Manuscript received May 28, 1981; revision received November 18, and accepted December 14, 1982.